Biomacromolecules

Article

pubs.acs.org/Biomac

In Vitro Toxicity Evaluation of Lignin-(Un)coated Cellulose Based Nanomaterials on Human A549 and THP-1 Cells

Naveena Yanamala,[†] Elena R. Kisin,[†] Autumn L. Menas,[†] Mariana T. Farcas,[†] Timur O. Khaliullin,[†] Ulla B. Vogel,[‡] Galina V. Shurin,[§] Diane Schwegler-Berry,[∥] Philip M. Fournier,[⊥] Alexander Star,[⊥] and Anna A. Shvedova*[,†,#]

[†]Exposure Assessment Branch/NIOSH/CDC, Morgantown, West Virginia 26505, United States

[‡]National Research Centre for the Working Environment, Copenhagen DK-2100, Denmark

[§]Department of Pathology, University of Pittsburgh Medical Center, Pittsburgh, Pennsylvania 15213, United States

[∥]Pathology & Physiology Research Branch/NIOSH/CDC, Morgantown, West Virginia 26505, United States

[⊥]Department of Chemistry, University of Pittsburgh, Pittsburgh, Pennsylvania 15213, United States

[#]Department of Physiology and Pharmacology, West Virginia University, Morgantown, West Virginia 26505, United States

Supporting Information

ABSTRACT: A significant amount of research toward commercial development of cellulose based nanomaterials (CNM) is now in progress with some potential applications. Using human A549 and THP-1 cells, we evaluated the biological responses of various CNMs, made out of similar material but with functional and morphological variations. While A549 cells displayed minimal or no cytotoxic responses following exposure to CNMs, THP-1 cells were more susceptible to cytotoxicity, cellular damage and inflammatory responses. Further analysis of these biological responses evaluated using hierarchical clustering approaches was effective in discriminating (dis)-similarities of various CNMs studied and identified potential inflammatory factors contributing to cytotoxicity. No correlation between cytotoxicity and surface properties of CNMs was found. This study clearly highlights that, in addition to the source and characteristics of CNMs, cell type-specific differences in the recognition/uptake of CNMs along with their inherent capability to respond to external stimuli are crucial for assessing the toxicity of CNMs.

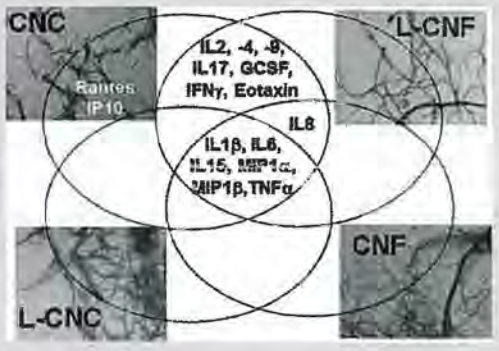

INTRODUCTION

In the field of nanotechnology, one of the most popular areas of current research and development, polymer-based nanocomposites, is gaining prominence in various industries such as transportation, construction, aerospace, and consumer products. Nanocomposite materials are the result of the combination of polymers and inorganic/organic fillers at the nanometer scale. The extraordinary versatility of these new materials springs from the large selection of nanofillers—nanoparticles, fibers, gels, minerals, and metals—being used for reinforcement and enhancing properties of base materials. In the recent years, cellulose-based nanomaterials (CNM) have received a great deal of attention because of their outstanding characteristics such as nanoscale dimension, high surface area, hydrophilicity, biodegradability and increased tensile strength, stiffness, and strain compared to other nanoscale materials.[1−3] CNMs can be produced from various sources including bacteria, wood, nonwoody plants and agricultural residues[4,5] and are extracted by two general methods: mechanical fibrillation and chemical hydrolysis.[6,7] The corresponding products are referred to as cellulose nanofibrils (CNF) and cellulose nanocrystals (CNC), respectively. While CNFs are fibrils and contain both amorphous and crystalline cellulosic regions, CNCs are stiff rod-like particles consisting of cellulose chain segments in a nearly perfect crystalline structure.[8] These novel CNMs are highly researched for their compatibility to serve as reinforcements in composites, replacing conventional materials such as glass fibers or inorganic fillers. However, the development of such high-performance nanocomposites requires surface functionalization and/or chemical modification of CNMs to overcome their intrinsic hydrophilic nature and attain uniform dispersions/distributions in polymer matrices.[9,10] The main challenge lies in preserving the original morphology and maintaining the integrity of the CNCs and CNFs. Several approaches including lignin-coating,[11−13] addition of surface charges, and surfactant or polymer grafting have been described to this end.[14−18] Relatively little is known about the potential effects of these CNMs on the environment

Received: May 24, 2016
Revised: September 16, 2016
Published: October 6, 2016

DOI: 10.1021/acs.biomac.6b00756
Biomacromolecules 2016, 17, 3464−3473

and on human health,[19] which is important given the increasing rates of their production and great potential for various applications.[3,20]

Research studies addressing the potential risk of inhalation exposure to CNCs are limited.[21−28] Several groups have investigated the cytotoxic effects of CNCs derived from several sources (wood, cotton, bacteria). While the majority of these studies have revealed no[29−31] or only minor indications of toxicity[24,29,32,33] of CNCs in the concentration range 0−50 μg/mL or up to 0.375 wt %, a dose-dependent cytotoxicity in *in vitro* studies for CNCs in the dose range 100−2000 μg/mL derived from cotton[34,35] and acute inflammatory responses in mice upon pharyngeal aspiration to CNFs[36] and CNCs[37,38] derived from wood at doses 50−240 μg/mouse was also observed. In some cases, despite no cytotoxic responses being found *in vitro*, a robust inflammatory response in mice was observed.[36] Nonetheless, the toxicological properties of CNF and CNC nanomaterials have been found to be greatly influenced by particle size, shape, structure as well as surface charge, chemistry and properties. These properties could in turn depend on the raw material source,[39] preprocessing of cellulose,[40] isolation procedures,[41] drying methods[42] and also on the type of surface functionalization/deposition techniques.[3,43,44] With the rapid increase in the development of novel CNCs and CNFs having important economic and technological advantages, it becomes crucial to systematically evaluate their safety before introducing them into the market.

The aim of this study was 2-fold: (a) to evaluate the cytotoxicity, cellular damage and inflammatory responses of CNCs and CNFs isolated from woody biomass sources,[12,13] and (b) to investigate whether the biological responses of lignin-coated (L-) hydrophobic forms of each type of CNMs are (dis-)similar to their uncoated hydrophilic forms. The different CNMs (CNC, L-CNC, CNF, L-CNF) employed in this study allowed for the consideration of the role of morphology (crystals vs fibrils) and surface properties (hydrophilic vs hydrophobic) in biological responses induced by CNCs and CNFs. The viability changes in A549 and THP-1 cells, representing alveolar epithelial type-II cells and macrophages, were systematically evaluated, following exposure to four different CNMs in the concentration range 5 μg/mL to 300 μg/mL for 24 and 72 h. The underlying mechanisms of cytotoxicity in each cell type were further investigated by assessing the release of lactate dehydrogenase (LDH) and various inflammatory cytokines in the cell culture supernatants. Finally, hierarchical clustering analysis was applied to determine and discriminate the cytotoxicity and inflammatory responses of the various CNMs in A549 and THP-1 cells. Studies such as this are essential for the development of future applications and safety assessment of CNMs and can stimulate more toxicologic evaluations of CNCs/CNFs and its derivatives. To the best of our knowledge, this is the first study that evaluated the toxicity responses of CNC and CNF compared to their lignin-coated forms isolated from woody biomass sources.[12,13]

■ EXPERIMENTAL SECTION

Materials. Microcrystalline cellulose (MCC, CAS. No: 9004−34−6) powder and lipopolysaccharides from *Escherichia coli* 0111:B4 (LPS, CAS. No: L2630) were purchased from Sigma-Aldrich (Saint Louis, MO). An UICC standard crocidolite asbestos (ASB) was used as a positive well-characterized fiber control. Freeze-dried powders of CNF and CNC materials as well as proprietary lignin-coated, hydrophobic varieties of each (L-CNC or L-CNF) were obtained from American Process Inc. (API), a company headquartered in Atlanta, Georgia. In the American Process AVAP Biorefinery pretreatment technology process, woody biomass is treated with sulfur dioxide and ethanol to produce the pulp that is then converted to CNC or CNF. Characteristics of the CNMs (CNC, CNF, L-CNC or L-CNF) used in the study are presented at API product specifications Web site (http://www.americanprocess.com/).

Methods. *Particle Preparation.* Four different types of CNMs, along with MCC as a negative control and LPS and ASB particles as positive controls, were employed in this study to compare and contrast their associated cellular toxicity. The various CNMs investigated included two types cellulose nanocrystals (CNC and L-CNC) and two cellulose nanofibrils (CNF and L-CNF). CNMs stock suspensions were made from freeze-dried powders obtained from API as well as ASB were prepared in United States Pharmacopeia (USP) grade water with pH adjusted to 7.0. The LPS stock suspensions were prepared using 1X phosphate buffered saline. These stock solutions were further diluted and sterilized by autoclaving and were briefly sonicated (30 s) with a probe sonicator (Branson Sonifer 450, 10W continuous output). Bacterial endotoxin levels were also measured using a Peirce LAL Chromogenic Endotoxin Quantitation kit according to the manufacturer's instructions (Thermo Fisher Scientific, MA). The endotoxin concentration in the particles was determined by extrapolating the absorbance at 405 nm against the standard curve (*E. coli* strain O11:B4 endotoxin supplied with kit). All particle suspensions had an endotoxin level below the detection limit (0.01 EU/ml). Each stock concentration was then serially diluted with corresponding type of medium for A549 and THP-1 cells to prepare desired test concentrations. A549 and THP-1 cells were then exposed to the same concentration range for each particle of interest (5, 10, 25, 50, 100, 200, 300 μg/mL) prepared in 1%-DMEM and 1%-RPMI medium, respectively.

Particle Characterization. Cellulose nanocrystal solutions were prepared by suspending the as-received solid samples in water. Transmission electron microscopy (TEM) of all CNMs along with MCC and ASB were performed using a JEOL 1220 TEM, by diluting the stock suspensions in double-distilled filtered water, the dispersion was then dropcast onto Formvar-coated copper grids and allowed to air-dry for detailed examination. Optical microscopy samples of all CNMs were prepared by drop casting 5 μL of 5 mg/L on freshly cleaved mica. An Olympus IX81 inverted system microscope was utilized for optical imaging, and ImageJ employed for image processing and particle area determination. Particle length was calculated by considering the measured area as a circle and its corresponding diameter. Only the smallest 75% of particles were considered in determining area and diameter averages. Atomic force microscopy (AFM) samples were made by drop casting 5 μL of 1 g/L sample solution on freshly cleaved mica. AFM was accomplished using a Multimode scanning probe microscope with a Nanoscope IIIa controller (Veeco) in tapping mode. An ACL probe (AppNano) was utilized at a frequency of 160−225 kHz, an amplitude set point of 1.70−1.75 V, and a drive amplitude of 100−300 mV. The resulting images were processed using the Gwyddion software tool.

Cell Culture and Exposure to CNMs. A549 cells (ATCC, CCL-185), a human lung carcinoma epithelial cell line, and THP-1 cells, a pro-monocytic cell line, were employed for testing the cytotoxicity of different nanoparticles employed in this study. The cytotoxic effects of each nanomaterial in A549 and THP-1 cell lines was tested at seven different concentrations ranging from 5−300 μg/mL. The highest dose investigated (300 μg/mL) in 100 μL of media would result in 0.0015 μg of deposited dose per cell (~2 million cells per 96 well-plate). A human equivalent workplace exposure to similar burden in alveolar macrophage and type-II cell can be achieved in ~5 and ~26 years, respectively[45,46] at allowable exposure limits (5 mg/m^3 of cellulose) defined by Occupational Safety & Health Administration (OSHA). These estimations included minute ventilation of 20 L/min and volume of 9.6 m^3/day (20 L/min × 0.001 m^3/L × 60 min/h × 8 h/day) for a person working a 8 h shift,[47] an alveolar deposition fraction of ~15%[48−51] based on aerodynamic particle size, and the total number of alveolar macrophages and Type-II epithelial cells of

DOI: 10.1021/acs.biomac.6b00756
Biomacromolecules 2016, 17, 3464−3473

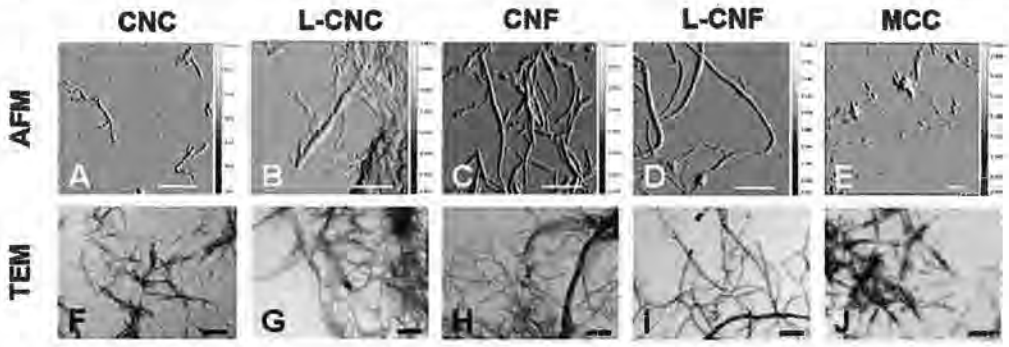

Figure 1. Characterization of nanocrystalline and microcrystalline cellulose samples. (A–E) AFM amplitude and (F–J) TEM images of CNC (A,F), L-CNC (B,G), CNF (C,H), L-CNF (D, I) and MCC (E,J). Scale bar in all AFM and TEM images corresponds to 500 and 200 nm, respectively.

5990 ± 1990 and 32 900 ± 13 600 million cells per lung for the humans.[52] For more details, please refer to the Supporting Information.

A549 cells were cultured in Dulbecco's Modified Eagle's Medium (DMEM) with 4.5 g/L glucose (Lonza, Alpharetta, GA) supplemented with 10% fetal bovine serum (FBS) (Atlanta Biologicals, Atlanta, GA), 1% L-glutamine (HyClone Life Technologies, Grand Island, NY), and 1% penicillin-streptomycin (PS) antibiotic (HyClone Life Technologies, Grand Island, NY) at 37 °C in 5% CO_2 humidified incubator.

THP-1 cells, were cultured in RPMI 1640 with L-glutamine and 25 mM Hepes (Lonza, USA) supplemented with 10% FBS (Atlanta Biologicals, Atlanta, GA), 0.05 mM 2-mercaptoethanol, and 1% PS at 37 °C in 5% CO_2 humidified incubator. Prior to seeding the cells in 96-well plates, THP-1 cells were differentiated with PMA (phorbol 12-myristate 13-acetate; Sigma-Aldrich, St. Louis, MO) at a concentration of 20 ng/mL in Roswell Park Memorial Institute (RPMI) 1640 + 10% FBS complete medium.

A549 and THP-1 cells were seeded into 96-well plates (Corning Incorporated Life Sciences, Tewksbury, MA), as a monolayer or at a nonconfluent cell density, 1 day prior to exposure under standard cell culture conditions in complete media. After allowing 24 h of cell attachment, plates were washed with 200 μL/well phosphate buffered saline and the cells were treated with increasing concentrations of each particle of interest prepared in 100 μL of clear (without phenol red) DMEM media containing 1% FBS + 1% L-glutamine +1% PS for 24 and 72 h. After 24 and 72 h incubation, the supernatants from each exposure and cell type were collected and frozen at −80 °C for later use in measuring cytokine release and lactate dehydrogenase activity. Cytotoxicity of A549 and THP-1 was assessed using alamar blue cell viability assay as outlined below.

AlamarBlue Cell Viability Assay. The alamarBlue assay was carried out according to manufacturer's instructions (ThermoFischer Scientific). Briefly, after 24 and 72 h of post exposure to control or test particles and removing supernatants the cells were rinsed with 100 μL/well of clear DMEM media, and 200 μL of alamarBlue solution (diluted 1:10 from stock solution) in fresh clear (without phenol red) DMEM media (without FBS or supplements) were added to each well. Following 3 h incubation at 37 °C, the cell viability was measured by quantifying alamarBlue fluorescence at the excitation (λ_{ex}) and emission (λ_{em}) wavelength of 485 and 595 nm, respectively. Wells containing medium and alamarBlue without cells were used as blanks. The mean fluorescent units of eight replicates per each particle and cell type were calculated, and the mean blank values were subtracted from them for each exposure treatment. The final results were expressed as relative viability of cells compared to that of control cells.

Quantification of LDH Activity. The activity of LDH in the cell free supernatants was assayed spectrophotometrically by monitoring the reduction of nicotinamide adenine dinucleotide at 340 nm in the presence of lactate using a Lactate Dehydrogenase Reagent kit (Pointe Scientific, Inc., Lincoln Park, MI).

Measurement of Cytokines/Chemokine/Growth Factors. The secretion and levels of various cytokine, chemokine, and growth factors in the cell free supernatants were determined by multiplex analysis using Bio-Plex Pro Human Cytokine 27-Plex Immunoassay kit (Bio-Rad Laboratories, CA, USA). This method simultaneously measures IL-1β, IL-1ra, IL-2, IL-4, IL-5, IL-6, IL-7, IL-8, IL-9, IL-10, IL-12 (p70), IL-13, IL-15, IL-17, IP-10, IFN-γ, MCP-1 (MCAF), MIP-1α, MIP-1β, PDGF-BB, RANTES, TNF-α, FGF basic, Eotaxin, G-CSF, GM-CSF, and VEGF. The principle of detection is based on an immunoassay configured on fluorescently dyed magnetic beads. Exactly 50 μL of A549 or THP-1 supernatants were used for the measurements of cytokines/chemokines/growth factors. Bio-Plex Manager 6.1 software (Bio-Rad, Tokyo) was used to estimate the concentration of each of the cytokine/chemokine/growth factors based on their respective standard curves.

Hierarchical Clustering Analysis Using R. Hierarchical agglomerative (bottom up) clustering analysis using the R statistical package[53] was applied to the control group and the samples corresponding to various concentrations of cellulose-based materials in THP-1 cells on the basis of their cytokine or cell viability responses at each post exposure time point investigated. A detailed cluster analysis of samples exposed to different types of CNMs (e.g., crystals vs fibrils, lignin-coated vs uncoated, micro vs nanocellulose) and other positive controls (e.g., LPS, ASB) was performed using "Euclidean" distance similarity between the different samples and by employing complete (largest) linkage distance between the members of the clusters. The dendrogram, in each case, was generated by the R[53] function hclust using a complete linkage clustering algorithm on Euclidean distance matrix.

Statistical Analysis. Results were compared by one-way ANOVA using the all pairwise multiple comparison procedures (Holm-Sidak method). All results are presented as mean + SEM P values of less than 0.05 were considered to indicate statistical significance.

RESULTS

Characterization of Lignin-Coated and Uncoated CNM Samples. Representative AFM and TEM images of cellulose-based samples investigated in this study are shown in Figure 1. Both techniques confirm the nanofibril architecture or high-aspect ratio morphology adopted by all samples with the exception of MCC. MCC exhibited a more amorphous morphology. AFM imaging only allowed for the observation of fibrils with nanoscale widths. Except for their size, the different CNM samples, CNC, L-CNC, CNF and L-CNF, were very similar. The AFM-based widths of CNC, L-CNC, CNF, L-CNF and MCC particles were 37 ± 7 nm, 47 ± 9 nm, 56 ± 14 nm, 48 ± 20 nm and 95 ± 41 nm, respectively. The TEM-based widths of CNC, L-CNC, CNF, and L-CNF particles were 20 nm, 20 nm, 50 nm, and 45 nm, respectively. Of the five CNMs investigated, MCC has the largest width, and CNC exhibited the smallest width, followed by L-CNC and L-CNF and then CNF. The particle lengths were not discernible using

DOI: 10.1021/acs.biomac.6b00756
Biomacromolecules 2016, 17, 3464–3473

either AFM or TEM. Because of the limited measurement view required to accurately measure nanoparticle widths, we employed optical microscopy (Table S1) to further assess the characteristics of these CNMs. The spot area and diameter, determined using optical microscopy, of CNC were smaller compared to CNF. When needle-shaped nonspherical nanoparticles, tumbling in the suspension, interact with light or cast a spot on the surface, the spot dimensions (area and diameter) correspond to the average length of the nanoparticles. The spot dimensions of the different CNMs investigated were in the order: L-CNF < MCC < CNC < L-CNC < CNF. Intriguingly, the measurement of L-CNC was more and L-CNF was less compared to CNC and CNF, respectively. From this it can be concluded that lignin coating decreases the average lengths of CNF particles and increases the spot dimensions of the CNC particles. This conclusion is further supported by the TEM studies. While L-CNF particles are found to appear more dispersed when dried on a TEM/AFM grid from aqueous solution compared to CNF, the dispersion of L-CNC is less compared to CNC (Figure 1). This suggests that depending on the CNM type and/or its morphology, lignin can lead to differential agglomeration/aggregation influencing their physicochemical properties in aqueous media.

Viability of A549 and THP-1 cells. The cell viability of A549 and THP-1 cells upon exposure to different CNMs was quantitatively determined using alamarBlue assay (Figure 2), in

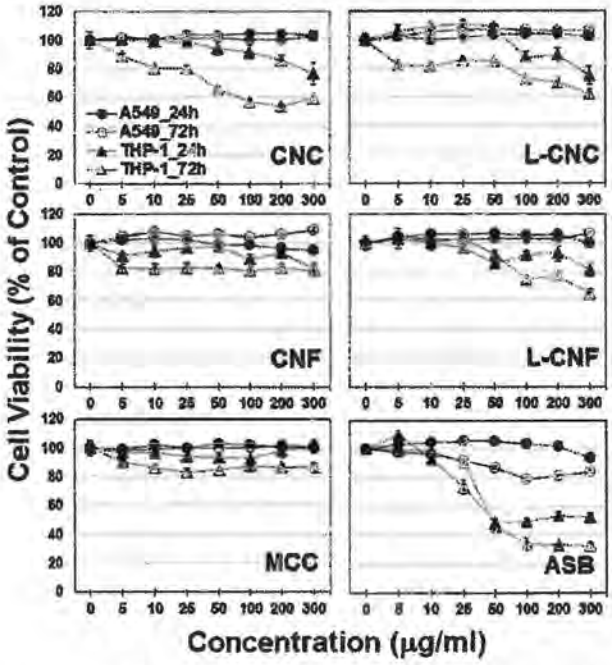

Figure 2. Viability of A549 and THP-1 cells after exposure to various concentrations of cellulose based nanomaterials for 24 and 72 h. The data are represented as Mean ± SEM ($n \geq 5$) of each sample.

which the conversion of the reagent resazurin to resorufin by metabolically active cells is detected based on fluorescence. While the viability loss in most cases is dose-related in THP-1 cells with the exception of CNF and MCC, the viability loss in A549 cells was only observed at high concentrations of ASB particles and at the 72 h post exposure time point. The effect of all cellulose nanomaterials on the viability of A549 cells was very little and was close to untreated (0 µg/mL) control cells in each case. Exposure to 300 µg/mL of ASB particles induced a viability loss of ~10% and ~20% after 24 and 72 h exposure, respectively, in A549 cells. Even at the highest concentration of 300 µg/mL, more than 90% of the A549 cells remain viable at both 24 and 72 h post exposure time points investigated. While the time point of exposure, with the exception of ASB particles, had little influence on the viability of A549 cells, THP-1 cells showed increased cytotoxicity after 72 h exposure to most of the particles compared to 24 h post exposure. At the highest concentration tested, exposure to CNC, L-CNC, CNF and L-CNF induced a cell viability loss of ~20% – 30% at 24 h post exposure. At 24 h post exposure, ASB particles (300 µg/mL) treated THP-1 cells were 55% viable. The viability loss at 72 h post exposure to 300 µg/mL concentration of different cellulose nanomaterials and ASB particles was as follows: ASB≫ CNC = L-CNC = L-CNF > CNF = MCC. Overall, these results clearly indicate that size and lignin-coating as well as the type of CNM are all factors that influence the viability in THP-1 cells. For A549 cells no viability loss related to any of the CNMs investigated, as determined using alamarBlue assay, was observed.

Membrane Integrity and Damage. The membrane damage of cells upon nanoparticle exposures leads to the release of the intracellular LDH into the cell culture medium. Therefore, LDH levels in the cell supernatants was used to assess the cell membrane integrity upon exposure to cellulose materials. The LDH levels in the cell culture medium of A549 and THP-1 cells at 72 h post exposure to various CNMs and ASB particles, estimated as percent of control, are shown in Figure 3 and listed in Table S2. No release of LDH was detected at 72 h post exposure to various cellulose-based

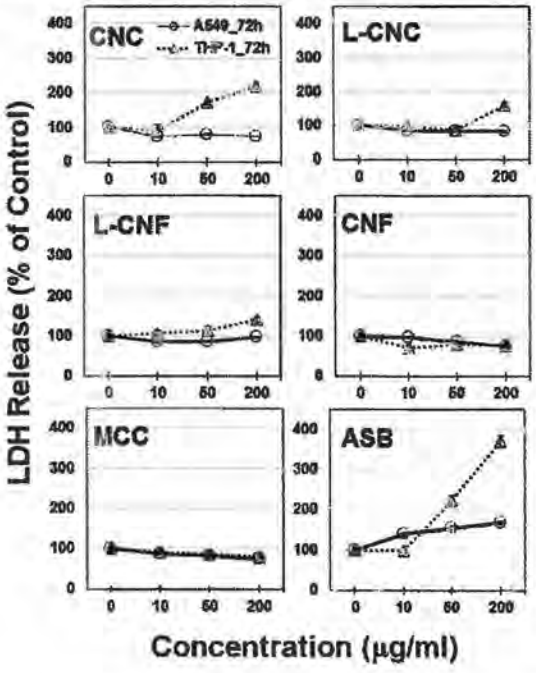

Figure 3. Cellular or membrane damage measured as lactate dehydrogenase (LDH) leakage in the supernatants of A549 and THP-1 cells after 72 h exposure. The data are represented as percent of control (Mean ± SEM, $n \geq 5$) of each exposed sample compared to the mean absolute values (U/L) from water-exposed controls.

DOI: 10.1021/acs.biomac.6b00756
Biomacromolecules 2016, 17, 3464–3473

materials in A549 cells. However, a dose-dependent increase in the LDH levels was found in A549 cells treated with ASB particles for 72 h (Figure 3). Exposure to even high concentrations of cellulose-based materials did not induce LDH leakage in A549 cells. In the case of THP-1 cells, the LDH levels of CNC and ASB treated cells showed a dose-dependent increase compared to the control cells (Figure 3). Exposure to 200 μg/mL of CNC and ASB particles in THP-1 cells induced an increase of ~119% and ~270% in the LDH levels after 72 h. Moreover, the LDH levels of lignin-coated cellulose nanomaterials were higher than that of control cells, albeit only at high concentrations tested. For example, at L-CNC and L-CNF concentration of 200 μg/mL, the LDH leakage level is increased by ~60% and 40%, respectively. Most importantly, the LDH levels of all of the different cellulose materials investigated in this study, with the exception of CNC in THP-1 cells, were lower in both A549 and THP-1 cells than that of the control cells (Figure 3 and Table S2). Overall, these results suggest a protective role of these materials against LDH leakage in both A549 and THP-1 cells, albeit with the exception of CNC and lignin-coated particles at high concentrations.

Inflammatory Cytokine Responses. In THP-1 cells, exposure to MCC, followed by L-CNC and then CNF had the overall least effect in inflammatory responses after both 24 and 72 h post exposure (Figure 4 and S2). After treating THP-1 cells for 24 h with 50 μg/mL of MCC or L-CNC or CNF, a significant increase in IL1β, MIP-1α, and MIP-1β levels was observed. In addition, exposing THP-1 cells to 50 μg/mL of L-CNC or CNF for 24 h also increased the levels of IL6 and IL15. Interestingly, none of the cytokines measured were found to be elevated after 72 h post exposure to MCC, CNF or L-CNC (Table S3). By contrast, exposure to CNC and L-CNF induced a robust inflammatory response both at 24 and 72 h compared to other cellulose-based materials investigated in this study. While treatment with 50 μg/mL of CNC or L-CNF for 24 h induced the increased levels of IL1β, IL2, IL4, IL6, IL8, IL9, IL15, IL17, GCSF, IFNγ, Eotaxin, MIP1α, MIP1β, and TNFα in THP-1 cells (Figure 4A and S2), an increase in additional cytokines including IL1Rα, IL10, IL13, and PDGF-BB was found after 72 h post exposure in THP-1 cells (Figure 4B). The significant increase observed in the levels of IP10 and Rantes at 24 and 72 h (Figure 4A) and the levels of IL5, IL7, MCP1 and FGF-basic at 72 h (Figure 4B) were unique to CNC-treated THP-1 cells compared to other cellulose-based particles. The inflammatory responses found upon exposure to CNC in THP-1 cells were similar to that of LPS (50 μg/mL) treatment in these cells (Table S3, S4). Overall the inflammatory responses in THP-1 cells upon exposure to different cellulose materials investigated were in the order: CNC > L-CNF > CNF $\geq$ L-CNC $\geq$ MCC.

Of the five different cellulose-based materials tested, exposure to MCC indicated the overall greatest effect in inflammatory responses in A549 cells both after 24 and 72 h post exposure (Figure 5). The only exception to this was that a significant increase in IL17 and FGF-basic levels was only observed after 24 h post exposure to L-CNC, CNF, and L-CNF (Figure 5A). However, the levels of IL8 and GM-CSF were found to be significantly increased in the A549 cell supernatants following 24 h post exposure to all cellulose particles tested. While the levels of the cytokines IL1Rα, IFNγ and MIP-1α were unique to MCC treated A549 cells after 24 h post exposure, an increase in in IL10 was observed upon exposure to both CNC and MCC (Figure 5A). In contrast the cytokine responses after treating A549 cells for 72 h with 50 μg/mL of CNC, L-CNC, CNF or L-CNF materials were much similar to MCC (Figure 5B). Interestingly, several cytokines including IL1Rα, IL8, IL9 and MIP-1α were similarly increased between different CNMs and MCC particles. In summary, the cytokine responses upon exposure to various cellulose-based materials, at the doses investigated in this study, were much less compared to the LPS treatment (positive control), in both A549 and THP-1 cells and at all post exposure time points (Table S4).

Hierarchical Clustering Analysis (HCA) of Cellular Toxicity and Inflammatory Responses in THP-1 Cells. HCA was applied to the data in Tables S3 and S4 to highlight the differences between the various cellulose-based material treatments in THP-1 cells. The dendrograms after 24 and 72 h post exposure to 50 μg/mL of CNC, L-CNC, CNF, L-CNF, MCC, and LPS are shown in Figure 6. Both dendrograms indicate that the Euclidean distance between CNC cluster and other treatments is quite large, clearly suggesting that the average cytokine responses after CNC exposure are quite different from the other cellulose materials studied. At 72 h a clear separation of CNC and L-CNF from the L-CNC, CNF, and MCC, in close clustering to the control group, was observed. While no clear separation of fibrils versus crystals or amorphous materials was observed at 72 h, the dendrogram at 24 h seems to separate CNF and L-CNF from L-CNC and MCC materials (Figure 6A). The distance of LPS treatment, a

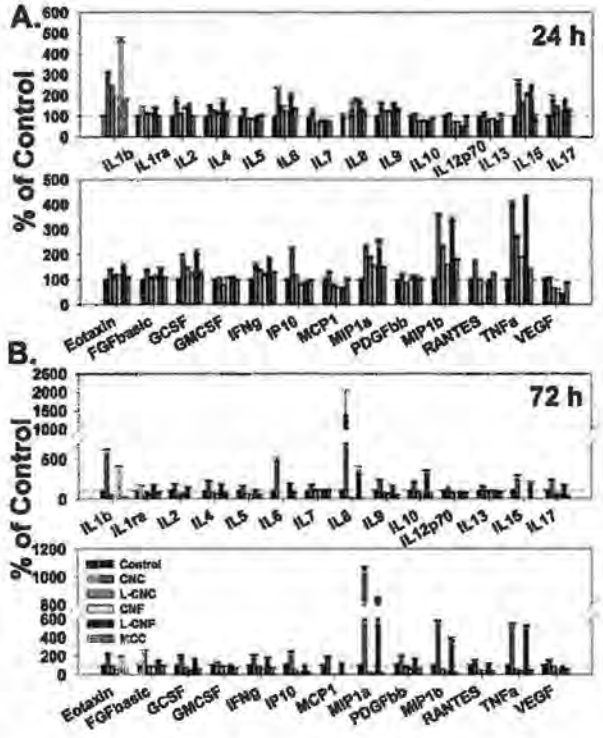

Figure 4. Cytokines and chemokines responses upon exposure to various cellulose based nanomaterials in THP-1 cells. The cytokines and chemokines levels at (A) 24 h and (B) 72 h post exposure to 50 μg/ml of various CNMs in the THP-1 cell supernatants. These measurements were performed using Bio-Plex Pro Human Cytokine 27-Plex Immunoassay kit, composed of a combination of pro- and anti-inflammatory cytokines with a subset of chemokines. The data is presented as percent change (Mean $\pm$ SEM, $n \geq 5$) compared to the mean absolute values from water-exposed controls.

DOI: 10.1021/acs.biomac.6b00756
Biomacromolecules 2016, 17, 3464−3473

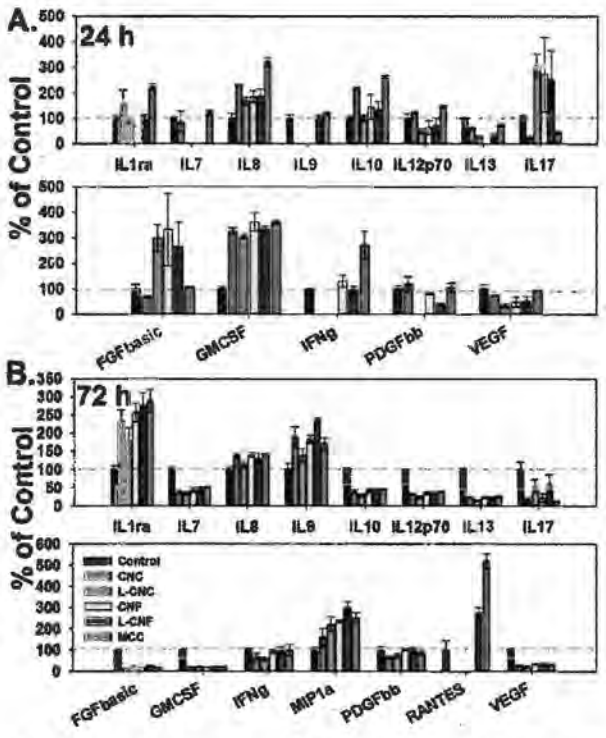

Figure 5. Cytokines and chemokines responses upon exposure to various cellulose based nanomaterials in A549 cells. The cytokines and chemokines levels at (A) 24 h and (B) 72 h post exposure to 50 μg/mL various CNMs in the A549 cell supernatants. These measurements were performed using Bio-Plex Pro Human Cytokine 27-Plex Immunoassay kit, composed of a combination of pro- and anti-inflammatory cytokines with a subset of chemokines. The data is presented as percent change (Mean $\pm$ SEM, $n \geq 5$) compared to the mean absolute values from water-exposed controls.

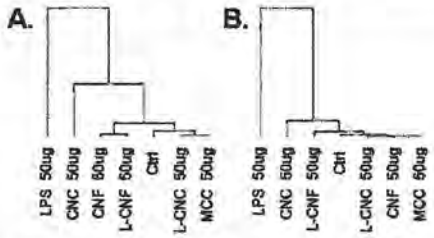

Figure 6. Hierarchical clustering analysis dendrograms of cytokine responses in THP-1 cells treated with different crystalline nano/micro-cellulose (CNC, L-CNC, MCC) and nanocellulose fiber (CNF, L-CNF) materials. The samples of THP-1 cells exposed to different concentrations of lignin-coated and uncoated CNC and NCF materials along with respective controls (MCC and LPS) were clustered based on the Euclidean distance metric and complete linkage clustering method at (A) 24 h and (B) 72 h post exposure time points. The samples in the dendrogram were reordered based on their (dis-)similarities in cytokines responses, measured in supernatants at each post exposure time point. Each branch in the dendrogram shows the similarity between samples, i.e., the shorter the branch, the more similar.

positive inflammatory control, from any of the clusters/treatment in THP-1 cells was large at both post exposure time points, clearly suggesting increased mean cytokine responses in THP-1 cells compared to all cellulose-based materials investigated as part of this study.

Additionally, the application of HCA to the cell viability responses also indicated similar clustering to that of cytokine responses (Figure S1). The resulting HCA dendrograms after 24 h post exposure to various concentrations (0, 25, 50, 100, 200, and 300 μg/mL) of CNC, L-CNC, CNF, L-CNF, MCC, crocidolite and LPS indicated a clear separation between all cellulose-based materials and the two positive controls, LPS and crocidolite (Figure S1, cluster in orange). In addition, the dendrogram further appears to separate the controls or no toxic treatments (Figure S1, green cluster) from cellulose-based material treatments, especially at high concentrations (Figure S1, blue cluster). Importantly at 72 h post exposure time point, all concentrations of CNC, with the exception of 25 μg/mL, along with L-CNF and L-CNC at the highest concentration tested were clustered together with LPS or ASB samples. Also, at 72 h post exposure, two major clusters separating controls and other cellulose-based particles (CNF, L-CNF, L-CNC, MCC) was observed, further suggesting a clear demarcation between untreated and cells treated with cellulose-based nanomaterials. All samples corresponding to CNF, L-CNC, and L-CNF particles at all concentrations (with the exception of highest concentration for lignin-coated materials) studied in THP-1 cells were clustered together with MCC, while CNC-based materials were found to be segregated with positive controls, in particular ASB. Moreover, the close clustering between CNC with either LPS and/or ASB particles clearly suggests that inflammatory and cell viability responses of CNCs can be unequivocally separated from other materials tested as part of this study. Overall, these results indicate that functional and morphological (dis)-similarities in CNMs could be determined based on their cytokine and cellular viability responses.

■ DISCUSSION

A large number of *in vivo/in vitro* studies reported, for the most part on cellulosic materials, were performed on a particular cell type or on a specific type of CNM.[22,29,30,34,35,39,54−56] Because of differences in experimental setup as well as processing/manufacturing procedures and sources of raw materials, it becomes difficult to compare and contrast the toxicity of various CNMs (e.g., crystals vs fibrils, wood vs algae vs cotton) resulting from such studies. Here, we evaluated and compared the toxicity of four different types CNMs all derived from woody biomass, having similar chemical composition but with different morphologies (fibrous vs crystalline) and/or coatings (uncoated vs lignin-coated), in A549 and THP-1 cells under equivalent experimental conditions. Overall results demonstrated that CNMs can elicit significant cytotoxic effects and increased inflammatory responses *in vitro*, albeit in a cell-type dependent manner and significantly less than the positive controls (e.g., ASB, LPS) at all concentrations considered in the current study.

Clear differences in the magnitude of cell viability and inflammatory responses in human THP-1 and A549 cells, representing the macrophages and alveolar-type-II cells in the lungs, was observed upon exposure to CNMs. Alveolar macrophages (MΦ) and alveolar epithelial cells act as the first line of defense against inhaled nanoparticles and play a key role in regulating inflammatory responses in the lungs. Of the two cell types studied, THP-1 cells exhibited pronounced cytotoxic and inflammatory responses upon exposure to CNMs.

DOI: 10.1021/acs.biomac.6b00756
Biomacromolecules 2016, 17, 3464−3473

While a dose-dependent cytotoxicity was seen in THP-1 cells, no significant cytotoxicity in A549 cells upon exposure to CNC, CNF, L-CNC, L-CNF, and MCC was found at used concentration/time points investigated (Figure 2). Additionally, the release of inflammatory cytokine responses in both cell types, upon exposure to various CNMs, were also in good agreement with cytotoxic responses (Figure 4 and 5 and Table S3). In particular, CNC nanoparticles induced a more robust inflammatory response compared to L-CNC, CNF, and L-CNF. The differential viability and inflammatory responses of the A549 and THP-1 cells reported in this study could be attributed to their different capacity of specific/nonspecific interactions with CNMs and their ability to respond to external stimuli. Most importantly, the function of phagocytosis that characterizes macrophage cells, but not alveolar epithelial cells, should be considered as a possibility that helps explain the higher sensitivity of THP-1 cells to CNMs. This possibility is further supported by previous studies that reported similar findings/conclusions in response to metal nanoparticles,[57] LPS,[58] and particulate matter exposures.[59] Despite the minimal response upon treating A549 cells with CNMs, it is important to understand the role of inflammatory mediators/factors released by THP-1 cells on A549 cells and their crucial role in the *in vivo* scenario, the entire lungs.

Of important note in this study is also that the biological responses following exposure to CNC and CNF nanomaterials are different than the response to CNMs upon lignin-coating in THP-1 cells. The comparison of the various CNMs employed revealed significant differences in the magnitude of the inflammatory or cytotoxic responses (Figure 2 and Table S3). In particular, compared to CNF, greater cytotoxicity and prominent increases in inflammatory cytokines were found upon exposure to CNC in THP-1 cells. The observation that CNF was less inflammatory can be correlated with CNF nanofibrils morphology compared to the crystalline/needle-like structure of CNC particles is inconsistent when their biological responses to their respective lignin-coated forms are considered. The inflammatory and cellular toxicity responses upon exposure to L-CNC, a hydrophobic lignin-coated form of CNC, were less prominent compared to L-CNF (Table S3, Figure 2), in contrast to what was observed for CNC and CNF materials. Also, a change in the nanoscale dimensions of both CNC and CNF materials was observed upon lignin-coating and indicated differential self-assembling and/or agglomeration upon dispersion in water and/or cell culture media. While lignin-coating increased the spot area and spot diameter of CNC particles indicating agglomeration, the dispersion of lignin-coated CNF particles in water decreased their particle dimensions (Table S1 and Figure 1). Nonetheless, the observed changes in biological responses upon exposure to various CNMs investigated, irrespective of lignin-coating, are in fact in good agreement with their overall relative nanoscale dimensions (Figure 1, S3 and Table S1). Overall, this study continues to support the notion that the toxicity of CNMs, in general, may be related to their physical-chemical-structural characteristics.[56] Even though other factors including media composition could play a significant role in CNM induced toxicity, the NP-dependent toxicity differences observed within each cell type highlights the importance of considering the physical-chemical-structural characteristics. It is important to note that the CNMs investigated in this study, despite their nanocrystalline structure, are much larger in their width compared to CNCs isolated from other sources such as wood, cotton, and bacteria.[37,60,61] Taken together, this study suggests that the association between CNM exposures and biological responses is complex and could be dependent on the type, size, and structure of CNMs and the specificity of cells to recognize and respond to them.[56]

A recent study reported an immunomodulatory potential of cellulose and demonstrated cellulose-mediated activation of toll-like receptor (TLR) dependent pathways, primarily involving TLR2 and TLR4 receptors, in THP-1 cells.[62] Of all the known TLRs, TLR4 acts as signal-transducing receptor for LPS, a Gram-negative bacterial cell wall component.[63−66] Upon treatment, LPS is shown to trigger a rapid inflammatory response through the release of several pro-inflammatory cytokines/chemokines including IL-1β, IL-6, IL-8, and TNFα.[18] Similarly, a time-dependent increase in the expression of IL-1β, IL-6, TNFα, and IL-8 in THP-1 cells, and IL-8 in A549 cells, along with other inflammatory mediators was also observed in this study. Most importantly, the found expression of IL1-β and TNFα in THP-1, but not in A549 cells, further validates and highlights their critical roles and mechanisms in regulating inflammatory/immune responses in the lungs. Both IL-1 and TNF-α act as potent inducers of chemokine production by many cell types, including pulmonary epithelial cells. While IL-8 triggers neutrophil migration, other chemokines such as RANTES, MCP-1 and MIP-1α/β—increased upon exposure to LPS in both A549 and THP-1 cells—trigger chemotactic and costimulatory effects on phagocytic and immune cells. Surprisingly, the overall inflammatory responses induced by CNMs (with the exception of MCC) in THP-1 cells, but not in A549 cells, indicated similarities to LPS, albeit to a much lesser extent at all doses investigated. Of note is also the close clustering of the overall biological responses of CNC and L-CNF to LPS at 72 h post exposure (Figure 6 and S1), highlighting the possibility that CNMs can be potential ligands for TLRs. LPS exposure induced decreased cell viability, increased cellular damage, and inflammatory responses in both A549 and THP-1 cells. However, these cellular changes were only observed for THP-1 cells in the case of CNMs (Figure 2). It is well-known that LPS recognition is through TLR4 mechanism and it is expressed in both THP-1 and A549 cells. Hence, no or low toxicity of CNMs in A549, compared to THP-1 cells, could be due to differences in the expression of TLR receptors and mechanisms that recognize LPS and other pathogen associated molecular patterns. Predominantly, CNMs have a repeating molecular pattern that is analogous, in many ways, to other TLR ligands such as chitin, β-glucans, mannans, and various microbial/fungal/plant cell wall components (Figure 7). In fact, a recent study demonstrated that biological responses to chitin (a polysaccharide found in fungi/insects/crustaceans) is mediated via MyD88-dependent and TLR2-dependent mechanisms and also revealed that chitin does not interact with TLR-4, further highlighting the specificity of TLR2 in recognizing chitin.[67] Based on the close structural resemblance of CNC to chitin fragments (Figure 7), we speculate that TLR2 receptors, and not TLR4, could play a key role in initiating biological responses of CNMs. Even though TLRs are the most extensively studied pattern recognition receptors (PRR), accumulating evidence also suggests that scavenger and C-type lectin PRRs play critical roles in the innate immune defense.[68−70] For example, the C-type lectin receptor, Dectin-1 collaborates with TLR2 to activate macrophages exposed to β-glucans[71] and chitin.[72] Thus, one cannot exclude the potential involvement of other cell surface PRRs,

DOI: 10.1021/acs.biomac.6b00756
Biomacromolecules 2016, 17, 3464−3473

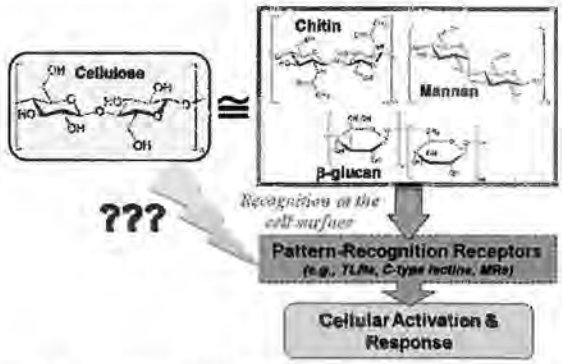

Figure 7. Schema highlighting the similarities in the repeating structural units of CNMs and other biological materials and suggesting the potential involvement of various surface pattern recognition receptors in recognizing the cellulose-based nanomaterials.

such as mannose and dectin receptors, for CNM recognition and regulation of inflammatory and/or immune responses (Figure 7). Further studies aimed at defining and exploring the functional interactions between different CNMs and the PRRs are needed to validate these notions.

CONCLUSIONS

In summary, this study demonstrates that the cytotoxic and inflammatory responses upon exposure to different CNMs, isolated from woody biomass, were cell-type specific and were further dependent on the type, size, and morphology of the CNMs. In contrast to A549 cells that indicated no or low toxicity to CNMs, exposure to CNMs, in particular CNC and L-CNF, elicited a dose-dependent cytotoxic and inflammatory responses in THP-1 cells. All CNMs at the doses investigated (5–300 μg/mL) as part of this study were found to be either nontoxic or less toxic compared to either fibrous ASB particles or to an inflammatory microbial cell wall component, LPS. In addition, the results comparing hydrophilic CNC or CNF with their respective hydrophobic lignin-coated forms, clearly showed differential agglomeration effects for each CNM type. Nonetheless, the data presented in this study indicates that, despite its biodurability and biocompatibility *in vivo*, CNCs can elicit adverse effects *in vitro*, albeit in a cell-type dependent manner. While in-depth toxicological studies employing sophisticated *in vitro* (e.g., 3D coculture models)[31] or *ex vivo* models is still required to assess the potential health effects associated with CNMs, the use of monocultures could still be useful to determine the role of each cell-type in triggering biological responses and their relevance in the lungs. Moreover, the findings presented are limited to the type of CNMs, cells and conditions investigated in this study, and great care should be taken when generalizing our findings to other CNC and CNF types, isolated from different sources and those employing different extraction and fabrication methods. The size, shape, aspect ratio, stiffness, and surface properties of CNMs can vary significantly depending on the raw material and production methods and can in turn influence their interactions with cells and subsequent biological responses (Figure S3). More studies that evaluate the mechanistic details of CNM interactions with cells[31,56] and that consider multiple target organ-specific cell types in parallel are necessary for understanding the toxicological profiles of CNCs and CNF exposures, and are currently underway.

ASSOCIATED CONTENT

Supporting Information

The Supporting Information is available free of charge on the ACS Publications website at DOI: 10.1021/acs.biomac.6b00756.

Additional description of the relevance of employed in vitro concentrations to realistic human exposures, specific cellulose staining in THP-1 cells, figures detailing hierarchical clustering analysis of cellular viability, Venn diagram representation of inflammatory responses, specific staining of cellulose materials in THP-1 cells upon exposure to CNMs, and additional tables listing optical microscopy based assessments of CNMs, cellular damage, and inflammatory cytokine/chemokine responses upon exposure to various CNMs, ASB and LPS (PDF)

AUTHOR INFORMATION

Corresponding Author

*Address: Exposure Assessment Branch (MS-3030), 1095 Willowdale Road, Morgantown, WV 26505 USA. Phone: (304) 285-6177. Fax: (304) 285-5938. E-mail: ats1@cdc.gov.

Funding

This work was supported by NIH R01ES019304, NIOSH 939051E, NTRC 939011K, and EC-FP-7-NANOSOLUTIONS.

Notes

The findings and conclusions in this report are those of the authors and do not necessarily represent the views of the National Institute for Occupational Safety and Health. Mention of trade names or commercial products do not constitute endorsement or recommendation for use.

The authors declare no competing financial interest.

REFERENCES

(1) Peng, B. L.; Dhar, N.; Liu, H. L.; Tam, K. C. Chemistry and Applications of Nanocrystalline Cellulose and Its Derivatives: A Nanotechnology Perspective. *Can. J. Chem. Eng.* **2011**, *89* (5), 1191–1206.

(2) Chinga-Carrasco, G.; Syverud, K. On the structure and oxygen transmission rate of biodegradable cellulose nanobarriers. *Nanoscale Res. Lett.* **2012**, *7*, 192.

(3) Kalia, S.; Dufresne, A.; Cherian, B. M.; Kaith, B. S.; Averous, L.; Njuguna, J.; Nassiopoulos, E. Cellulose-Based Bio- and Nanocomposites: A Review. *Int. J. Polym. Sci.* **2011**, *2011*, 837875.

(4) Syverud, K.; Chinga-Carrasco, G.; Toledo, J.; Toledo, P. G. A comparative study of Eucalyptus and Pinus radiata pulp fibres as raw materials for production of cellulose nanofibrils. *Carbohydr. Polym.* **2011**, *84* (3), 1033–1038.

(5) Zimmermann, T.; Bordeanu, N.; Strub, E. Properties of nanofibrillated cellulose from different raw materials and its reinforcement potential. *Carbohydr. Polym.* **2010**, *79* (4), 1086–1093.

(6) Spence, K. L.; Venditti, R. A.; Rojas, O. J.; Habibi, Y.; Pawlak, J. J. A comparative study of energy consumption and physical properties of microfibrillated cellulose produced by different processing methods. *Cellulose* **2011**, *18* (4), 1097–1111.

(7) Mtibe, A.; Linganiso, L. Z.; Mathew, A. P.; Oksman, K.; John, M. J.; Anandjiwala, R. D. A comparative study on properties of micro and nanopapers produced from cellulose and cellulose nanofibres. *Carbohydr. Polym.* **2015**, *118*, 1–8.

(8) Atalla, R. H. L. *The individual structures of native celluloses.* 10th International Symposium on Wood and Pulping Chemistry, Main Symposium, 1999 June 07-10, Yokohama, Japan; TAPPI Press: Atlanta, GA, 1999; pp 608–614.

DOI: 10.1021/acs.biomac.6b00756
Biomacromolecules 2016, 17, 3464–3473

(9) Eyley, S.; Thielemans, W. Surface modification of cellulose nanocrystals. *Nanoscale* **2014**, *6* (14), 7764−79.
(10) Habibi, Y.; Lucia, L. A.; Rojas, O. J. Cellulose nanocrystals: chemistry, self-assembly, and applications. *Chem. Rev.* **2010**, *110* (6), 3479−500.
(11) TUNC, M. S.; Pylkkanen, V.; Retsina, T. *Lignin-coated cellulose fibers from lignocellulosic biomass*.WO 2015126583 A1, 2015.
(12) Nelson, K.; Retsina, T. Innovative nanocellulose process breaks the cost barrier. *TAPPI Journal* **2014**, *13* (5), 19−23.
(13) Nelson, K.; Retsina, T.; Pylkkanen, V.; O'connor, R. *Processes and apparatus for producing nanocellulose, and compositions and products produced therefrom*. US 20140154757 A1, 2015
(14) Leung, A. C.; Hrapovic, S.; Lam, E.; Liu, Y.; Male, K. B.; Mahmoud, K. A.; Luong, J. H. Characteristics and properties of carboxylated cellulose nanocrystals prepared from a novel one-step procedure. *Small* **2011**, *7* (3), 302−5.
(15) Zaman, M.; Xiao, H.; Chibante, F.; Ni, Y. Synthesis and characterization of cationically modified nanocrystalline cellulose. *Carbohydr. Polym.* **2012**, *89* (1), 163−70.
(16) Zhang, K.; Sun, P.; Liu, H.; Shang, S.; Song, J.; Wang, D. Extraction and comparison of carboxylated cellulose nanocrystals from bleached sugarcane bagasse pulp using two different oxidation methods. *Carbohydr. Polym.* **2016**, *138*, 237−43.
(17) Carlmark, A.; Larsson, E.; Malmström, E. Grafting of cellulose by ring-opening polymerisation − A review. *Eur. Polym. J.* **2012**, *48* (10), 1646−1659.
(18) Segura, M.; Vadeboncoeur, N.; Gottschalk, M. CD14-dependent and -independent cytokine and chemokine production by human THP-1 monocytes stimulated by Streptococcus suis capsular type 2. *Clin. Exp. Immunol.* **2002**, *127* (2), 243−54.
(19) Shatkin, J. A.; Kim, B. Cellulose nanomaterials: life cycle risk assessment, and environmental health and safety roadmap. *Environ. Sci.: Nano* **2015**, *2* (5), 477−499.
(20) Roman, M. Toxicity of Cellulose Nanocrystals: A Review. *Ind. Biotechnol.* **2015**, *11* (1), 25−33.
(21) Lin, N.; Dufresne, A. Nanocellulose in biomedicine: Current status and future prospect. *Eur. Polym. J.* **2014**, *59*, 302−325.
(22) Adamis, Z.; Tatrai, E.; Honma, K.; Ungvary, G. In vitro and in vivo assessment of the pulmonary toxicity of cellulose. *J. Appl. Toxicol.* **1997**, *17* (2), 137−141.
(23) Cullen, R. T.; Miller, B. G.; Clark, S.; Davis, J. M. G. Tumorigenicity of cellulose fibers injected into the rat peritoneal cavity. *Inhalation Toxicol.* **2002**, *14* (7), 685−703.
(24) Kovacs, T.; Naish, V.; O'Connor, B.; Blaise, C.; Gagne, F.; Hall, L.; Trudeau, V.; Martel, P. An ecotoxicological characterization of nanocrystalline cellulose (NCC). *Nanotoxicology* **2010**, *4* (3), 255−70.
(25) Roman, M.; Dong, S. P.; Hirani, A.; Lee, Y. W. Cellulose Nanocrystals for Drug Delivery. *ACS Symp. Ser.* **2010**, *1017*, 81−91.
(26) Tatrai, E.; Adamis, Z.; Bohm, U.; Meretey, K.; Ungvary, G. Role of cellulose in wood dust-induced fibrosing alveo-bronchiolitis in rat. *J. Appl. Toxicol.* **1995**, *15* (1), 45−8.
(27) Tatrai, E.; Brozik, M.; Adamis, Z.; Meretey, K.; Ungvary, G. In vivo pulmonary toxicity of cellulose in rats. *J. Appl. Toxicol.* **1996**, *16* (2), 129−35.
(28) Warheit, D. B.; Snajdr, S. I.; Hartsky, M. A.; Frame, S. R. Two-week inhalation study in rats with cellulose fibers. *Int. Congr Ser.* **1998**, *1153*, 579−582.
(29) Ni, H.; Zeng, S.; Wu, J.; Cheng, X.; Luo, T.; Wang, W.; Zeng, W.; Chen, Y. Cellulose nanowhiskers: preparation, characterization and cytotoxicity evaluation. *Biomed Mater. Eng.* **2012**, *22* (1−3), 121−7.
(30) Dong, S.; Hirani, A. A.; Colacino, K. R.; Lee, Y. W.; Roman, M. CYTOTOXICITY AND CELLULAR UPTAKE OF CELLULOSE NANOCRYSTALS. *Nano LIFE* **2012**, *02* (03), 1241006.
(31) Endes, C.; Schmid, O.; Kinnear, C.; Mueller, S.; Camarero-Espinosa, S.; Vanhecke, D.; Foster, E. J.; Petri-Fink, A.; Rothen-Rutishauser, B.; Weder, C.; Clift, M. J. An in vitro testing strategy towards mimicking the inhalation of high aspect ratio nanoparticles. *Part. Fibre Toxicol.* **2014**, *11*, 40.
(32) Yang, X.; Bakaic, E.; Hoare, T.; Cranston, E. D. Injectable polysaccharide hydrogels reinforced with cellulose nanocrystals: morphology, rheology, degradation, and cytotoxicity. *Biomacromolecules* **2013**, *14* (12), 4447−55.
(33) Cullen, R. T.; Searl, A.; Miller, B. G.; Davis, J. M.; Jones, A. D. Pulmonary and intraperitoneal inflammation induced by cellulose fibres. *J. Appl. Toxicol.* **2000**, *20* (1), 49−60.
(34) Pereira, M. M.; Raposo, N. R.; Brayner, R.; Teixeira, E. M.; Oliveira, V.; Quintao, C. C.; Camargo, L. S.; Mattoso, L. H.; Brandao, H. M. Cytotoxicity and expression of genes involved in the cellular stress response and apoptosis in mammalian fibroblast exposed to cotton cellulose nanofibers. *Nanotechnology* **2013**, *24* (7), 075103.
(35) Clift, M. J.; Foster, E. J.; Vanhecke, D.; Studer, D.; Wick, P.; Gehr, P.; Rothen-Rutishauser, B.; Weder, C. Investigating the interaction of cellulose nanofibers derived from cotton with a sophisticated 3D human lung cell coculture. *Biomacromolecules* **2011**, *12* (10), 3666−73.
(36) Rouhiainen, J.; Väänänen, V.; Tsitko, I.; Kautto, J. Risk assessment of nanofibrillated cellulose in occupational settings. In *SUNPAP Final Conference*, Milan, Italy, 2012.
(37) Yanamala, N.; Farcas, M. T.; Hatfield, M. K.; Kisin, E. R.; Kagan, V. E.; Geraci, C. L.; Shvedova, A. A. Evaluation of the Pulmonary Toxicity of Cellulose Nanocrystals: A Renewable and Sustainable Nanomaterial of the Future. *ACS Sustainable Chem. Eng.* **2014**, *2* (7), 1691−1698.
(38) Shvedova, A. A.; Kisin, E. R.; Yanamala, N.; Farcas, M. T.; Menas, A. L.; Williams, A.; Fournier, P. M.; Reynolds, J. S.; Gutkin, D. W.; Star, A.; Reiner, R. S.; Halappanavar, S.; Kagan, V. E. Gender differences in murine pulmonary responses elicited by cellulose nanocrystals. *Part. Fibre Toxicol.* **2015**, *13* (1), 28.
(39) de Lima, R.; Oliveira Feitosa, L.; Rodrigues Maruyama, C.; Abreu Barga, M.; Yamawaki, P. C.; Vieira, I. J.; Teixeira, E. M.; Correa, A. C.; Caparelli Mattoso, L. H.; Fernandes Fraceto, L. Evaluation of the genotoxicity of cellulose nanofibers. *Int. J. Nanomed.* **2012**, *7*, 3555−65.
(40) Chinga-Carrasco, G.; Syverud, K. Pretreatment-dependent surface chemistry of wood nanocellulose for pH-sensitive hydrogels. *J. Biomater. Appl.* **2014**, *29* (3), 423−432.
(41) Qing, Y.; Sabo, R.; Zhu, J. Y.; Agarwal, U.; Cai, Z.; Wu, Y. A comparative study of cellulose nanofibrils disintegrated via multiple processing approaches. *Carbohydr. Polym.* **2013**, *97* (1), 226−34.
(42) Peng, Y.; Gardner, D. J.; Han, Y. Drying cellulose nanofibrils: in search of a suitable method. *Cellulose* **2012**, *19* (1), 91−102.
(43) Beck-Candanedo, S.; Roman, M.; Gray, D. G. Effect of reaction conditions on the properties and behavior of wood cellulose nanocrystal suspensions. *Biomacromolecules* **2005**, *6* (2), 1048−54.
(44) Usov, I.; Nystrom, G.; Adamcik, J.; Handschin, S.; Schutz, C.; Fall, A.; Bergstrom, L.; Mezzenga, R. Understanding nanocellulose chirality and structure-properties relationship at the single fibril level. *Nat. Commun.* **2015**, *6*, 7564.
(45) Erdely, A.; Dahm, M.; Chen, B. T.; Zeidler-Erdely, P. C.; Fernback, J. E.; Birch, M. E.; Evans, D. E.; Kashon, M. L.; Deddens, J. A.; Hulderman, T.; Bilgesu, S. A.; Battelli, L.; Schwegler-Berry, D.; Leonard, H. D.; McKinney, W.; Frazer, D. G.; Antonini, J. M.; Porter, D. W.; Castranova, V.; Schubauer-Berigan, M. K. Carbon nanotube dosimetry: from workplace exposure assessment to inhalation toxicology. *Part. Fibre Toxicol.* **2013**, *10* (1), 53.
(46) NIOSH *Current Intelligence Bulletin: Occupational Exposure to Carbon Nanotubes and Nanofibers*; U.S. Department of Health and Human Services, Public Health Service, Centers for Disease Control, National Institute for Occupational Safety and Health: Cincinnati, OH, 2010; pp DHHS (NIOSH) Docket Number: NIOSH 161-A; available at http://www.cdc.gov/niosh/docket/review/docket161A/.
(47) Galer, D. M.; Leung, H. W.; Sussman, R. G.; Trzos, R. J. Scientific and practical considerations for the development of occupational exposure limits (OELs) for chemical substances. *Regul. Toxicol. Pharmacol.* **1992**, *15* (3), 291−306.
(48) *Multiple Path Particle Dosimetry Model (MPPD v 1.0): A Model for Human and Rat Airway Particle Dosimetry*; National Institute for

DOI: 10.1021/acs.biomac.6b00756
Biomacromolecules 2016, 17, 3464−3473

Public Health and the Environment (RIVM): Bilthoven, The Netherlands, 2002.
(49) Anjilvel, S.; Asgharian, B. A multiple-path model of particle deposition in the rat lung. *Fundam. Appl. Toxicol.* **1995**, *28* (1), 41−50.
(50) Bates, D. V.; Fish, B. R.; Hatch, T. F.; Mercer, T. T.; Morrow, P. E. Deposition and retention models for internal dosimetry of the human respiratory tract. Task group on lung dynamics. *Health Phys.* **1966**, *12* (2), 173−207.
(51) ICRP. Human Respiratory Tract Model for Radiological Protection. *Ann. ICRP* **1994**, *24*, 1−3.
(52) Stone, K. C.; Mercer, R. R.; Gehr, P.; Stockstill, B.; Crapo, J. D. Allometric relationships of cell numbers and size in the mammalian lung. *Am. J. Respir. Cell Mol. Biol.* **1992**, *6* (2), 235−43.
(53) R Core Team, *R: A language and environment for statistical computing*; R Foundation for Statistical Computing: Vienna, Austria, 2014.
(54) Mahmoud, K. A.; Mena, J. A.; Male, K. B.; Hrapovic, S.; Kamen, A.; Luong, J. H. Effect of surface charge on the cellular uptake and cytotoxicity of fluorescent labeled cellulose nanocrystals. *ACS Appl. Mater. Interfaces* **2010**, *2* (10), 2924−32.
(55) Kollar, P.; Zavalova, V.; Hosek, J.; Havelka, P.; Sopuch, T.; Karpisek, M.; Tretinova, D.; Suchy, P., Jr. Cytotoxicity and effects on inflammatory response of modified types of cellulose in macrophage-like THP-1 cells. *Int. Immunopharmacol.* **2011**, *11* (8), 997−1001.
(56) Endes, C.; Mueller, S.; Kinnear, C.; Vanhecke, D.; Foster, E. J.; Petri-Fink, A.; Weder, C.; Clift, M. J.; Rothen-Rutishauser, B. Fate of cellulose nanocrystal aerosols deposited on the lung cell surface in vitro. *Biomacromolecules* **2015**, *16* (4), 1267−75.
(57) Lanone, S.; Rogerieux, F.; Geys, J.; Dupont, A.; Maillot-Marechal, E.; Boczkowski, J.; Lacroix, G.; Hoet, P. Comparative toxicity of 24 manufactured nanoparticles in human alveolar epithelial and macrophage cell lines. *Part. Fibre Toxicol.* **2009**, *6*, 14.
(58) Hara, S., Ishimatsu, Y.; Mukae, H.; Sakamoto, N.; Kakugawa, T.; Fujita, H.; Hara, A.; Kohno, S. Anti-inflammatory effects of garenoxacin on IL-8 production and ERK1/2 activation induced by lipopolysaccharides in A549 and THP-1 cells. *Eur. J. Pharmacol.* **2011**, *668* (1−2), 264−70.
(59) Riley, M. R.; Boesewetter, D. E.; Turner, R. A.; Kim, A. M.; Collier, J. M.; Hamilton, A. Comparison of the sensitivity of three lung derived cell lines to metals from combustion derived particulate matter. *Toxicol. In Vitro* **2005**, *19* (3), 411−9.
(60) George, J.; Sabapathi, S. N. Cellulose nanocrystals: synthesis, functional properties, and applications. *Nanotechnol., Sci. Appl.* **2015**, *8*, 45−54.
(61) Hanif, Z.; Ahmed, F. R.; Shin, S. W.; Kim, Y. K.; Um, S. H. Size- and dose-dependent toxicity of cellulose nanocrystals (CNC) on human fibroblasts and colon adenocarcinoma. *Colloids Surf., B* **2014**, *119*, 162−5.
(62) Vogt, L. M.; Boekschoten, M. V.; de Groot, P. J.; Faas, M. M.; de Vos, P. Cellulose alters the expression of nuclear factor kappa B-related genes and Toll-like receptor-related genes in human peripheral blood mononuclear cells. *J. Funct. Foods* **2015**, *18*, 520−531.
(63) Beutler, B. Inferences, questions and possibilities in Toll-like receptor signalling. *Nature* **2004**, *430* (6996), 257−63.
(64) Chow, J. C.; Young, D. W.; Golenbock, D. T.; Christ, W. J.; Gusovsky, F. Toll-like receptor-4 mediates lipopolysaccharide-induced signal transduction. *J. Biol. Chem.* **1999**, *274* (16), 10689−92.
(65) Palsson-McDermott, E. M.; O'Neill, L. A. Signal transduction by the lipopolysaccharide receptor, Toll-like receptor-4. *Immunology* **2004**, *113* (2), 153−62.
(66) Tapping, R. I.; Akashi, S.; Miyake, K.; Godowski, P. J.; Tobias, P. S. Toll-like receptor 4, but not toll-like receptor 2, is a signaling receptor for Escherichia and Salmonella lipopolysaccharides. *J. Immunol.* **2000**, *165* (10), 5780−7.
(67) Da Silva, C. A.; Hartl, D.; Liu, W.; Lee, C. G.; Elias, J. A. TLR-2 and IL-17A in chitin-induced macrophage activation and acute inflammation. *J. Immunol.* **2008**, *181* (6), 4279−86.
(68) Gordon, S. Pattern recognition receptors: doubling up for the innate immune response. *Cell* **2002**, *111* (7), 927−30.
(69) Akira, S.; Uematsu, S.; Takeuchi, O. Pathogen recognition and innate immunity. *Cell* **2006**, *124* (4), 783−801.
(70) Mukhopadhyay, S.; Gordon, S. The role of scavenger receptors in pathogen recognition and innate immunity. *Immunobiology* **2004**, *209* (1−2), 39−49.
(71) Gantner, B. N.; Simmons, R. M.; Canavera, S. J.; Akira, S.; Underhill, D. M. Collaborative induction of inflammatory responses by dectin-1 and Toll-like receptor 2. *J. Exp. Med.* **2003**, *197* (9), 1107−17.
(72) Da Silva, C. A.; Chalouni, C.; Williams, A.; Hartl, D.; Lee, C. G.; Elias, J. A. Chitin is a size-dependent regulator of macrophage TNF and IL-10 production. *J. Immunol.* **2009**, *182* (6), 3573−82.

DOI: 10.1021/acs.biomac.6b00756
Biomacromolecules 2016, 17, 3464−3473